573

Egypt. J. Chem. **Vol. 66,** No. 12, pp. 251 - 259 (2023)

Egyptian Journal of Chemistry

Effect of Isopropyl Myristate and Oleic Acid as the Penetration Enhancer on Transdermal Patch Loaded Meloxicam Solid Dispersion: Characteristics and *In-Vitro* Diffusion

Nining Nining, Anisa Amalia, Novrina Maharani, Siti Robiatul Adawiyah

Department of Pharmaceutical Technology, Faculty of Pharmacy and Science, Universitas Muhammadiyah Prof. Dr. Hamka, Jakarta 13460, Indonesia

Abstract

The transdermal drug delivery system (TDDS) delivers meloxicam (MX) that can reduce the adverse effects of orally administered MX with a chemical enhancer. Solid dispersion of meloxicam is used to help increase its solubility. Chemical penetration enhancers interact with skin components to enhance drug molecule flux. This study examines how isopropyl myristate (IPM) and oleic acid (OA), as penetration enhancers, affect the characteristics of transdermal patches and MX diffusion in-vitro. Patches with IPM (1-10% b/b) or OA (5-20% b/b) were prepared, and their characteristics were compared with patches without enhancers. The patches' physical appearance, weight variance, thickness, folding endurance, and pH were all evaluated. For drug-carrier compatibility in the solid dispersion, FTIR investigations were carried out; the Franz diffusion cell was utilized to examine *in-vitro* diffusion characteristics. Patch characteristics obtained were weight variance of 482 ± 2.78 to 541 ± 1.49 mg; thickness 0.85 ± 0.02 to 0.94 ± 0.01 mm; drug content 99.1 ± 1.2 to $99.7\pm0.6\%$; folding endurance >300; pH 5.22 ± 0.02 to 5.45 ± 0.02. The MX permeated from IPM-MX and OA-MX patches showed the highest flux, at 83.789 $\mu m/cm^2 h$ and 84.405 $\mu m/cm^2 h$, respectively. The data suggest that OA can be applied as a penetration enhancer for transdermal administration of MX through matrix-type patches. The most effective enhancer was OA, which had an excellent diffusion flux of 84.405 $g/cm^2 h$, cumulative MX permeated of 720.50 ± 1.93 $\mu g/cm^2$, and an enhancement ratio of 1.070 with negative lag time.

Keywords: Controlled release formulation; Kinetics; Chemical penetration enhancer; Anti-Inflammatory agents; Drug delivery systems.

1. Introduction

Meloxicam (MX), an oxicam derivative, is a selective inhibitor of cyclooxygenase-2 (COX-2) and a nonsteroidal anti-inflammatory drug (NSAID) [1]. The MX dosage can be delivered at only 7.5 mg daily in the long-term treatment of ankylosing spondylitis and rheumatoid arthritis in the elderly [2]. However, MX's gastrointestinal adverse drug reaction profile was reported to be similar to other NSAIDs [1]. The molecular weight of MX, 4-hydroxy-2 methyl-N-(5-methyl-2-thiazolyl)-2H-1,2-benzothiazine3-carboxamide-1,1-dioxide, is 351.4 [3], coefficient partition (log P) 3.43 [4], $pKa_1 = 1.1$ (hydroxyl group) and $pKa_2 = 4.2$ (thiazole group), and a half-life of 15-20 hours [2]–[6]. MX, like other NSAIDs, is practically insoluble in water, and solubility in solutions of pH 1.2 or 4.0 is low, ca. 0.6 g/mL [3], [5], [6]. Solid dispersions formation can increase the solubility of MX and its bioavailability [7], [8].

A transdermal drug delivery system (TDDS) delivers MX that can reduce the adverse effects of orally administered MX. Skin delivery of NSAIDs effectively avoids GI adverse effects, improves patient compliance, and remains safe [9]–[12]. Because of its minimal tissue toxicity, MX can be administered to the skin and mucosa [13]. Other advantages of TDDS are to avoid hepatic metabolism, release drugs for a long time, and

_____

provide convenience in drug administration and drug discontinuation in the event of toxicity [14], [15]. However, drug delivery is limited because drug molecules must pass through the stratum corneum barrier sequentially to penetrate deeper layers of the skin [16]. Chemical penetration enhancers interact with skin components to enhance drug molecule flux [17].

The advantages of using chemical penetration enhancers over physical penetration enhancers include design flexibility, simplicity of application, patient compliance, the ability to self-administer and extend medication release through patches, and their inclusion into low-cost and accessible formulas [18]. Esters and fatty acid groups were utilized as chemical penetration enhancers in this research. Isopropyl myristate (IPM), an ester penetration enhancer, is the most common and widely used in commercial products [19]. The mechanism of action is to integrate the lipid layer to increase the fluidity of the skin, soften the rigid skin structure, and increase the diffusion coefficient and drug permeation [18], [20]. Oleic acid (OA) is a fatty acid group that can increase drug penetration by producing a permeable defect in SC lipids due to oleic acid's cis double bond. That enables it to deliquesce itself rather than disperse uniformly in natural skin fats [18], [19], [21]–[23].

In this study, we developed the solid dispersion of meloxicam (SDMX) loading transdermal patch for better anti-inflammatory management therapy. Furthermore, this study assists in determining the penetration-enhancing effect of the patch matrix on the in vitro drug release. A patch matrix composed of hydrophilic and hydrophobic polymers created a system to control and maintain drug release [24], [25].

2. Experimental
2.1. Materials

MX was purchased from Apex Healthcare Ltd. (India); IPM (BASF, Germany); ethyl cellulose/ EC (Asha Cellulose (I) PVT. LTD., India); HPMC 60SH-10000 (Shin-Etsu, Japan); glycerine (Wilmar Nabati, Indonesia); PEG 6000 (Pan Asia Chemical, Taiwan); and OA (Avantor). All of the other substances utilized were from the pharmaceutical grade.

2.2. SDMX Preparation

PEG 6000 was melted at $70 \pm 5°C$ and mixed with MX (ratio 8:1). The mixture was rapidly cooled in an ice bath. Then, the solid dispersion was stored for 24 hours in a desiccator at room temperature and sieved through mesh 80 [26].

2.3. SDMX Characterization

SD characterization includes FTIR and MX contents. The FTIR (Agilent Technologies Carry 630) test was carried out by inserting SD into the sample holder and then compressing it. The spectrum was analyzed in the 4000-650 cm^{-1} wavenumber range [27]. MX contents were determined spectrophotometrically following Bolourchian et al. [28] with modifications. MX and SD were carefully weighed and mixed in pH 7.4 phosphate buffer, followed by 5 min of sonication until dissolved. MX contents were measured at a wavelength of 362 nm using UV-Vis spectrophotometry (Shimadzu UV-1900).

2.4. Preparation of Transdermal Patch

Transdermal patch formula can be seen in Table 1. Transdermal patches were prepared by solvent evaporation technique where ethyl cellulose (EC) dissolves with ethanol, and HPMC dissolves with methanol. The two polymer solutions were mixed and stirred until homogeneous. Glycerine and enhancer were added and stirred into the polymer mixture. Lastly, SDMX was added and stirred until homogeneous. Afterward, the mixture was poured into the mold provided and dried at room temperature for two days. After drying, the patches were cut into 10 cm^2 squares, covered in aluminum foil, and kept in a desiccator [29].

Table 1: MX Transdermal Patch Formula

Materials	Formula (%$^w/_w$)						
	1	2	3	4	5	6	7
SD*	13,75	13,75	13,75	13,75	13,75	13,75	13,75
EC	27	27	27	27	27	27	27
HPMC	12	12	12	12	12	12	12
IPM	-	1	5	10	-	-	-
OA	-	-	-	-	5	10	20
Glycerine	28	28	28	28	28	28	28
Solvents** ad	100	100	100	100	100	100	100

* Equivalent to 7.5 mg of meloxicam per patch
** Methanol: ethanol ratio of 1: 2

2.5. Transdermal Patch Characterization
2.5.1. Visual observation and pH testing

Visual observations include shape, odor, surface conditions, and color. The pH test was conducted by soaking a patch with 10 mL of distilled water for 2-h. Three times measurements were taken with a calibrated pH meter (Hanna) [30].

2.5.2. Determination of drug content

The determination followed the method of Mahajan et al. [29] with modifications. Patch size 10 cm^2 was dissolved in ethanol and stirred with a magnetic stirrer for 60 min. The solution was filtered

_____

into a 50 mL volumetric flask with ethanol. Next, the solution was pipetted 1 mL and adjusted into a 10 mL measuring flask. Furthermore, a UV-Vis spectrophotometer (Shimadzu UV-1900) was used to measure absorbance at a wavelength of 363 nm.

2.5.3. Patch thickness and weight uniformity

The thickness test was carried out in triplicate by measuring a patch at three points using a screw micrometer (Tricle Brand). The weight uniformity test was carried out in triplicate by weighing ten randomly selected patches. The weighing process was done with an analytical balance (Ohaus). The measurement data has calculated the average and standard deviation [29].

2.5.4. Folding endurance

Folding endurance testing was carried out by repeatedly folding the patch at the same spot until damage occurred. The procedure was repeated three times, and the number of folds completed was recorded as the folding endurance value [29].

2.6. Permeation Studies
2.6.1. Membrane impregnation time optimization

Synthetic nitrocellulose membrane (MF-Millipore Merck, 0.22 m, thickness 150 μm) was impregnated with Spangler's solution. The solution was prepared by melting a mixture of 5% stearic acid, 5% cholesterol, 5% squalene, 10% palmitic acid, 10% liquid paraffin, 15% oleic acid, 15% coconut oils, 15% white vaseline, and 20% olive oil. The membrane was immersed in the solution for 10, 30, 45, and 60 min, and then the percentage increase in membrane weight after impregnation was calculated. The time the membrane reaches a constant weight was set as the optimum time [31].

2.6.2. In-vitro diffusion studies

This test used a Franz diffusion cell (PermeGear, Inc. Hellertown, AP, USA). A synthetic membrane divided the cylinder into two compartments, the donor compartment and the receptor compartment. The receptor compartment was kept at 37 ± 0.5°C. Diffusion media in a 15 mL phosphate buffer pH 7.4 solution stirred with a magnetic stirrer. A sample port was located next to the receptor compartment [32]. Diffusion was performed for 8-h, and 1 mL of receptor solution was taken at 30, 60, 90, 120, 180, 240, 300, 360, 420, and 480-min intervals for spectrophotometric measurement at 362 nm. Following the sampling, the same volume of receptor solution was introduced to the receptor compartment. The concentration of substances diffused was determined by sample analysis [33].

2.6.3. Data analysis

The cumulative amount of permeated drugs (Q) is plotted as a time function [34]. X-intercept and slope of the linear graph between the amount permeated and time are used to determine lag time and flux, respectively. Permeation parameters determined by the method stated by Jafri et al. [35], such as flux, permeability coefficient (a), lag time, enhancement ratio (b), diffusion coefficient (c), regression coefficient, and best-fit equation.

$P = J/C$ … (a)

where P is permeation, J is the flux, and C is the drug concentration in patch.

$ER = J_{PE}/J_{control}$ … (b)

where ER is enhancement ratio, J_{PE} is the flux of patch containing permeation enhancer, and $J_{control}$ is flux of patch without permeation enhancer.

$DC = h^2/6L$ … (c)

where DC is diffusion coefficients, h is thickness of membran, and L is lag time.

3. Results and Discussion
3.1. Meloxicam Solid Dispersion Preparation

Solid dispersions were prepared by fusing MX and PEG 6000. Hydrophilic carriers in solid dispersions have been widely reported to increase the solubility and dissolution of MX [26], [36]; PEG 6000 is an amorphous polymer carrier that produces a second-class solid dispersion type [37]. The composition of the solid dispersion of MX-PEG 6000 with a ratio of 1:8 is known to have no chemical interactions. It can increase the solubility of MX and good release profile [26]. The melting method was carried out by directly heating the physical mixture between the drug and carrier until it melts at a temperature above its melting point. The advantage of this method is a simple and economical process [37]. The solid dispersion was in the form of yellow powder with a yield of 81.12%. MX content was determined spectrophotometrically with a phosphate buffer with pH 7.4 and a maximum wavelength of 362 nm. The linear regression equation for the calibration curve obtained is y=0.0207x+0.0106, with a value of r=0.9993. The MX content in SD was 10.91 ± 0.08%.

Figure 1 presents the FTIR spectra of solid dispersions and their single compounds. Spectrum 1c shows that the MX crystals appear trapped in the carrier particles. The functional group peaks observed in 1c are similar to 1a with the differential of several peaks whose intensity decreased, namely N-H at 3289.4 cm^{-1}; C=O at 1619.5 cm^{-1}; C=N at 1530.1 cm^{-1} and 1550.6 cm^{-1}; and S=O at 1183 cm^{-1}. This observation indicates the possibility of hydrogen bonding through the N-H, C=O, C=N, and S=O groups in the MX and PEG 6000 hydroxyl groups, also reported in other studies [27]. Several fingerprint peaks at 1466,7 to 840,5 cm^{-1} in 1c with
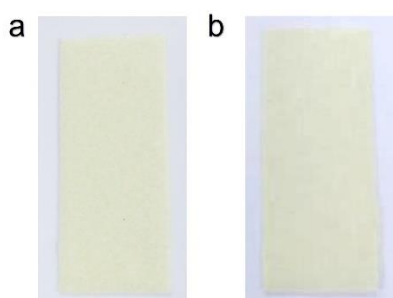
decreased intensity compared to spectrum 1b with unchanged peak characteristics, suggesting that even though the drug molecule and polymer form hydrogen bonds, the overall group on the drug molecule does not change. Moreover, other studies reported that there is no interaction between carrier and drug where no overlap or merge of spectral peaks was identified [26], [36].

3.2. Transdermal Patch Characteristics

Organoleptically, the patch is rectangular and odorless with a dry, uncracked, flat surface condition with a yellow color scattered throughout the surface (Figure 2). The yellow color apprs from

the MX content and indicates the homogeneity of the MX dispersion in the patch. The MX patches characterize, and the outcomes are presented in Table 2. The mean weights of F1-7 ranged from 482±2.78 mg to 541±1.49 mg, and the percent drug content ranged from 99.1±1.2 to 99.7±0.6%. The results of the various formula's specific weights are similar to drug content with a 90-110% specific range. The similarity in weight and content uniformity indicates that the preparation method is efficient in producing patches with low variations in drug content and can be utilized to generate an MX matrix-type patch commercially.

Figure 1: FTIR test results (a) MX (b) PEG 6000 (c) SD

Figure 2: Visual observation (a) IPM-MX patch and (b) OA-MX patch

Patch thickness ranged from 0.85±0.02 mm to 0.94±0.01 mm. The increase in patch weight and thickness (F2-F4 for an IPM-MX patch; F5-F7 for an OA-MX patch) could be seen with increasing enhancer concentration. It may be because the EC used as the polymer matrix has low water permeability properties that prevent the evaporation of water and other volatile compounds, thereby retaining significant mass [29]. In determining the concentration of MX in the patch, the measurement of the MX maximum absorption in 96% ethanol solvent was carried out at a wavelength of 363 nm, the same as in other studies [38]. The standard curve linear regression equation obtained is y=0.045x-0.0008 with a value of r=0.9998.

As a mechanical evaluation, folding endurance was performed manually to determine patch plasticity. The folding endurance value is calculated by the number of times the film can be folded in the exact location without breaking. The results showed that the patch had a folding endurance value of more than 300 folds, with the patch being in a good condition, not damaged, and not cracked. Thus, using glycerine as a plasticizer provides good flexibility to the patch.

Patch pH ranged from 5.22±0.02 to 5.45±0.02. The patch pH value was compatible with the skin pH value of about 5.4-6.9 and it is appropriate for topically administered [39]. Furthermore, considering that MX has a $pKa_1 = 1.1$ and $pKa_2 = 4.2$ [2], [5], the drug is not ionized at this pH, making it optimal for penetration into the stratum corneum [39]. Table 2 shows the decrease in pH from F2-F4 and F5-F7 when the enhancer concentration increased; F4 and F7, Each formula's pH value satisfies the 4.5–6.5 standards for skin pH [40].

Formula 7, which uses oleic acid to enhance penetration, has the lowest pH of all the formulations. These results are consistent with investigations by Aliyah et al., [41], which demonstrated that the pH of the formulations decreased as oleic acid concentrations increased.

3.3. MX Release Diffusion Rate

The *in-vitro* drug that released assays from topical preparations was carried out to characterize the final product's performance as a quality assessment method and justify post-approval alterations and scale-up [42]. Vertical diffusion cells are an *in-vitro* test model for predicting bioavailability and bioequivalence by measuring drug release from semisolid and transdermal dosage forms [9,22–24]. This release test can use synthetic membranes, such as nitrocellulose. Permeation studies with synthetic membranes can be used as an initial screening with good reliability [43]. Synthetic membranes are preferred over biological membranes because they are easier to obtain, have a simpler structure with uniform thickness, and are cheaper, so their use in large-scale studies can be done more easily. At the same time, the mechanism can be deconvolved more easily [44], [45]. Nitrocellulose membranes usage, one of four synthetic membranes, in a drug release test from creams has shown good acceptability. It may provide useful information for developing regulatory guidelines for biowaivers [32]. Its membrane is less hydrophobic [32], so it needs immersion with a spangler solution. The membrane impregnation time optimizes by immersing the membrane in a spangler solution—optimum time selection based on the membrane's weight that has the smallest weight increase [46]. The optimum result of membrane impregnation is at 10 min.

A diffusion test was performed using a Franz diffusion cell with a nitrocellulose membrane with a pore diameter of 0.22 m impregnated with Spangler's solution. The receptor compartment is filled with a pH 7.4 phosphate buffer solution, which serves as a substitute for simulating the pH conditions of the body's biological fluids. The cumulative amount of diffused MX increased steadily and gradually over time (Figure 3).
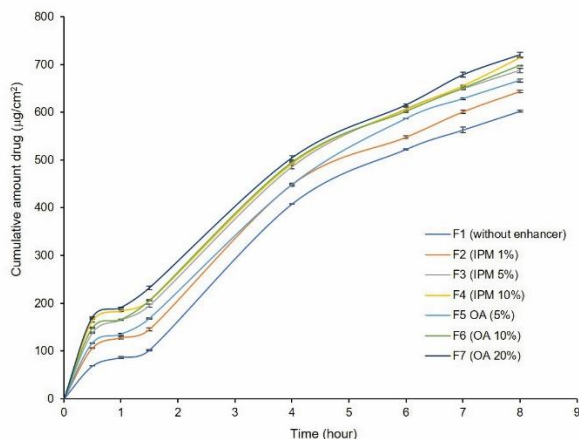
Table 2: MX matrix-type patch characterization

Formula	Mean ± SD (*n*=3)				
	Drug content (%)	Thickness (mm)	Weight (mg)	Folding endurance	pH
1	99.5±0.8	0.85±0.02	482±2.78	>300	5.45±0.02
2	99.6±0.6	0.88±0.01	488±4.48	>300	5.38±0.01
3	99.5±0.2	0.90±0.02	504±3.54	>300	5.33±0.02
4	99.6±0.2	0.92±0.02	521±2.58	>300	5.29±0.02
5	99.4±0.2	0.86±0.02	508±2.28	>300	5.41±0.02
6	99.1±1.2	0.90±0.03	523±2.85	>300	5.31±0.01
7	99.7±0.6	0.94±0.01	541±1.49	>300	5.22±0.02

Figure 3: *In-vitro* syntetic membrane permeation profile of MX from transdermal patches (n = 3). Vertical bar represents standard deviation.

In the presence of IPM (F2-F4) and OA (F5-F7) in the patch, when compared to the control formula (F1), MX permeation was significantly enhanced (Figure 3). When IPM and OA were added, a synergistic effect of MX permeation from the patch through the membrane was observed. The cumulative MX permeated from the IPM-MX patch (F2-4) at 8-h was 643.56±4.87 µg/cm^2, 687.11±0.62 µg/cm^2, and 714.14±3.75 µg/cm^2, respectively. Meanwhile, the cumulative amount of MX permeated from the OA-MX patch (F5-7) at 8-h was 666.24±0.33 µg/cm^2, 697.72±1.33 µg/cm^2, and 720.50±1.93 µg/cm^2, respectively. In this study, the cumulative amount of permeated MX was higher in the IPM-MX patch than OA-MX patch. A similar finding founded in the heparin sodium permeation transdermal IPM patch and OA patch [23]. Flux is calculated by dividing the cumulative amount of permeated drug per cm2 of the membrane by time [35]. F7, containing the highest OA, showed maximum permeated at 8-h with the most considerable flux of 84.405 g/cm^{2}h with an enhancement ratio (ER) of 1.070 (Table 3). The ranking order of the effects of enhancement MX permeation from the patch is F7 > F4 > F3 > F6 > F5

> F2 > F1. As a penetration enhancer, OA can be an effective method for lowering the skin's barrier function. Many NSAIDs are shown to enhance percutaneous absorption by adding OA [22]. OA interacts with stratum corneum lipids and alters their structure, increasing fluidity as a reaction of flux [19], [22]. The reaction of OA with lipids in stratum corneum reduces the lipid glass transition and promotes drug penetration; it also lowers the lipid viscosity of the superficial layer [35]. Touitou et al. investigated the morphology of epidermal Langerhans cells in response to several penetration enhancers. They concluded that OA significantly impacts skin morphology, increasing penetration throughout the skin [47]. IPM can be partitioned into the skin's polar phase (protein) because it is semi-polar and tends to enhance the drug's partition coefficient for the skin, thereby enhancing its diffusivity to the skin [48].

Table 3 shows the permeation parameters of all patches. In our study, all lag times were negative (extrapolation results of linear plots Figure 3), both on patches with and without enhancers. This result does not have physical meaning but indicates that enhancer presence significantly reduces the phase lag time. IPM 10% (F4) and 20% OA (F7) formulations showed higher permeability with shorter time lags. Similar findings were found in geraniol permeation with 5% N-acetyl-L-cysteine enhancer [49] and diclofenac sodium solution [50], which showed high permeability with a negative lag time. Mathematically, the negative lag time is caused by the high drug permeation at the first sampling point, and the flux has reached a steady state [49]. A negative intercept is very common when the initial pressure increase is slow, and drug permeation is high, so the time for the pressure to rise and reach a steady state is comparable [51]. From the third sample point, the same phenomena can be seen in MX permeation (1.5 hours) (Figure 3). When the lag time method is used to calculate the diffusion coefficient (D) from experimental data, the number is negative, which is also not physically meaning [51].

Table 3: Permeation parameters of MX patch transdermal where *J* is flux, *P* is permeation coefficient, *L* is lag time, *DC* is diffusion coefficient, and *ER* is enhancement ratio.

Permeation parameters	J (µm/cm^{2}h)	Intercept	R^2	P (cm/h)	L (h)	DC (cm^2/h)	ER
F1 (without enhancer)	78.9	17.891	0.9767	0.1662	-0.23	-0.00017	1.000
F2 (IPM 1%)	80.306	46.479	0.9742	0.1690	-0.58	-6.5E-05	1.018
F3 (IPM 5%)	83.726	72.689	0.9684	0.1764	-0.87	-4.3E-05	1.061
F4 (IPM 10%)	83.789	84.293	0.9681	0.1764	-1.01	-3.7E-05	1.062
F5 (OA 5%)	83.098	52.879	0.9774	0.1753	-0.64	-5.9E-05	1.053
F6 (OA 10%)	83.594	78.051	0.9670	0.1770	-0.93	-4,00E-05	1.059
F7 (OA 20%)	84.405	93.884	0.9647	0.1776	-1.11	-3,40E-05	1.070

4. Conclusions

Based on the results of the study, it can be concluded that the use of IPM and OA as penetration enhancers is able to produce transdermal patches with physical properties that meet the requirements and increase cumulative MX permeated, flux, and permeation coefficient. The data suggest that OA can be applied as a penetration enhancer for transdermal administration of MX through matrix-type patches. The most effective enhancer was OA, which had the most excellent diffusion flux of 84.405 g/cm^2h, cumulative MX permeated of 720.50 ± 1.93 $\mu g/cm^2$, and an enhancement ratio of 1.070 with negative lag time.

5. Conflicts of Interest

There are no declared conflicts.

6. Acknowledgments

7. References

[1] J. K. Aronson, Ed., "Meloxicam," in *Meyler's Side Effects of Drugs*, 16th ed., Oxford, United Kingdom: Elsevier, 2015, pp. 819–821.

[2] N. Y. Khalil and K. F. Aldosari, "Meloxicam," *Profiles Drug Subst. Excipients Relat. Methodol.*, vol. 45, pp. 159–197, 2020, doi: 10.1016/bs.podrm.2019.10.006.

[3] *British Pharmacopoeia Vol. II*. London, United Kingdom: Her Majesty's Stationary Office, 2016.

[4] National Center for Biotechnology Information, "PubChem Compound Summary for CID 54677470: Meloxicam," 2021. .

[5] M. Ochi *et al.*, "Physicochemical and Pharmacokinetic Characterization of Amorphous Solid Dispersion of Meloxicam with Enhanced Dissolution Property and Storage Stability," *AAPS PharmSciTech*, vol. 17, no. 4, pp. 932–939, 2016, doi: 10.1208/s12249-015-0422-x.

[6] P. R. Nassab, R. Rajkó, and P. Szabó-Révész, "Physicochemical characterization of meloxicam-mannitol binary systems," *J. Pharm. Biomed. Anal.*, vol. 41, no. 4, pp. 1191–1197, 2006, doi: 10.1016/j.jpba.2006.02.055.

[7] M. Jafar, D. MHG, and A. Shareef, "Enhancement of Dissolution and Anti-inflamatory effect of Meloxicam Using Solid Dispersions," *Int. J. Appl. Pharm.*, vol. 2, no. 1, pp. 22–27, 2010.

[8] Y. C. Ah, J. K. Choi, Y. K. Choi, H. M. Ki, and J. H. Bae, "A novel transdermal patch incorporating meloxicam: In vitro and in vivo characterization," *Int. J. Pharm.*, vol. 385, no. 1–2, pp. 12–19, 2010, doi: 10.1016/j.ijpharm.2009.10.013.

[9] C. Zeng *et al.*, "Relative efficacy and safety of topical non-steroidal anti-inflammatory drugs for osteoarthritis: A systematic review and network meta-analysis of randomised controlled trials and observational studies," *Br. J. Sports Med.*, vol. 52, no. 10, pp. 642–650, 2018, doi: 10.1136/bjsports-2017-098043.

[10] G. Honvo *et al.*, "Safety of Topical Non-steroidal Anti-Inflammatory Drugs in Osteoarthritis: Outcomes of a Systematic Review and Meta-Analysis," *Drugs and Aging*, vol. 36, no. s1, pp. 45–64, 2019, doi: 10.1007/s40266-019-00661-0.

[11] C. A. Heyneman, C. Lawless-Liday, and G. C. Wall, "Oral versus topical NSAIDs in rheumatic diseases: A comparison," *Drugs*, vol. 60, no. 3, pp. 555–574, 2000, doi: 10.2165/00003495-200060030-00004.

[12] B. S. Galer, M. Rowbotham, J. Perander, A. Devers, and E. Friedman, "Topical diclofenac patch relieves minor sports injury pain: Results of a multicenter controlled clinical trial," *J. Pain Symptom Manage.*, vol. 19, no. 4, pp. 287–294, 2000, doi: 10.1016/S0885-3924(00)00125-1.

[13] P. Stei, B. Kruss, J. Wiegleb, and V. Trach, "Local tissue tolerability of meloxicam, a new NSAID: Indications for parenteral, dermal and mucosal administration," *Br. J. Rheumatol.*, vol. 35, no. SUPPL. 1, pp. 44–50, 1996, doi: 10.1093/rheumatology/35.suppl_1.44.

[14] S. Amodwala, P. Kumar, and H. P. Thakkar, "Statistically optimized fast dissolving microneedle transdermal patch of meloxicam: A patient friendly approach to manage arthritis," *Eur. J. Pharm. Sci.*, vol. 104, no. 51, pp. 114–123, 2017, doi: 10.1016/j.ejps.2017.04.001.

[15] R. Kumar and A. Philip, "Modified Transdermal Technologies: Breaking the Barriers of Drug Permeation via the Skin," *Trop. J. Pharm. Res.*, vol. 6, no. 1, pp. 633–644, 2007, doi: 10.4314/tjpr.v6i1.14641.

[16] S. M. Sammeta, M. A. Repka, and S. N. Murthy, "Magnetophoresis in combination with chemical enhancers for transdermal drug delivery," *Drug Dev. Ind. Pharm.*, vol. 37, no. 9, pp. 1076–1082, 2011, doi: 10.3109/03639045.2011.559659.

[17] A. C. Williams and B. W. Barry, "Penetration enhancers," *Adv. Drug Deliv. Rev.*, vol. 64, no. SUPPL., pp. 128–137, 2012, doi: 10.1016/j.addr.2012.09.032.

[18] N. Dragicevic and H. I. Maibach, "Percutaneous penetration enhancers chemical

methods in penetration enhancement: Modification of the stratum corneum," *Percutaneous Penetration Enhanc. Chem. Methods Penetration Enhanc. Modif. Strat. Corneum*, pp. 1–411, 2015, doi: 10.1007/978-3-662-47039-8.

[19] M. E. Lane, "Skin penetration enhancers," *Int. J. Pharm.*, vol. 447, no. 1–2, pp. 12–21, 2013, doi: 10.1016/j.ijpharm.2013.02.040.

[20] K. Ita, *Transdermal Drug Delivery: Concepts and Application*, 1th ed. Academic Press, 2020.

[21] J. Choi, M. K. Choi, S. Chong, S. J. Chung, C. K. Shim, and D. D. Kim, "Effect of fatty acids on the transdermal delivery of donepezil: In vitro and in vivo evaluation," *Int. J. Pharm.*, vol. 422, no. 1–2, pp. 83–90, 2012, doi: 10.1016/j.ijpharm.2011.10.031.

[22] J. S. Baek, J. H. Lim, J. S. Kang, S. C. Shin, S. H. Jung, and C. W. Cho, "Enhanced transdermal drug delivery of zaltoprofen using a novel formulation," *Int. J. Pharm.*, vol. 453, no. 2, pp. 358–362, 2013, doi: 10.1016/j.ijpharm.2013.05.059.

[23] R. P. Patel, D. R. Gaiakwad, and N. A. Patel, "Formulation, optimization, and evaluation of a transdermal patch of heparin sodium," *Drug Discov. Ther.*, vol. 8, no. 4, pp. 185–193, 2014, doi: 10.5582/ddt.2014.01030.

[24] C. Valenta and B. G. Auner, "The use of polymers for dermal and transdermal delivery," *Eur. J. Pharm. Biopharm.*, vol. 58, no. 2, pp. 279–289, 2004, doi: 10.1016/j.ejpb.2004.02.017.

[25] S. Raza *et al.*, "Design, preparation and evaluation of meloxicam transdermal patches using flaxseed/coriander oils as penetration enhancers," *Lat. Am. J. Pharm.*, vol. 37, no. 11, pp. 2298–2311, 2018.

[26] V. S. Shenoy and S. Pandey, "Meloxicam-PEG 6000 solid dispersions in rapidly disintegrating tablets : preparation , in vitro and in vivo characterization," *Asian J. Pharm. Sci.*, vol. 3, no. 4, pp. 142–150, 2008.

[27] S. G. Vijaya Kumar and D. N. Mishra, "Preparation, characterization and in vitro dissolution studies of solid dispersion of meloxicam with PEG 6000 1," *Yakugaku Zasshi*, vol. 126, no. 8, pp. 657–664, 2006, doi: 10.1248/yakushi.126.657.

[28] N. Bolourchian, M. Nili, S. M. Foroutan, A. Mahboubi, and A. Nokhodchi, "The use of cooling and anti-solvent precipitation technique to tailor dissolution and physicochemical properties of meloxicam for better performance," *J. Drug Deliv. Sci. Technol.*, vol. 55, no. September 2019, p. 101485, 2020, doi: 10.1016/j.jddst.2019.101485.

[29] N. M. Mahajan, G. H. Zode, D. K. Mahapatra, S. Thakre, N. Dumore, and P. S. Gangane, "Formulation development and evaluation of transdermal patch of piroxicam for treating dysmenorrhoea," *J. Appl. Pharm. Sci.*, vol. 8, no. 11, pp. 35–41, 2018, doi: 10.7324/JAPS.2018.81105.

[30] L. Nurdianti, T. Rusdiana, I. Sopyan, N. A. Putriana, H. R. Aiman, and T. R. Fajria, "Characteristic comparison of an intraoral thin film containing astaxanthin nanoemulsion using sodium alginate and gelatin polymers," *Turkish J. Pharm. Sci.*, vol. 18, no. 3, pp. 289–295, 2021, doi: 10.4274/tjps.galenos.2020.25483.

[31] R. P. Tofani, Y. C. Sumirtapura, and S. T. Darijanto, "Formulation, characterisation, and in vitro skin diffusion of nanostructured lipid carriers for deoxyarbutin compared to a nanoemulsion and conventional cream," *Sci. Pharm.*, vol. 84, no. 4, pp. 634–645, 2016, doi: 10.3390/scipharm84040634.

[32] S. Nallagundla, S. Patnala, and I. Kanfer, "Comparison of in vitro release rates of acyclovir from cream formulations using vertical diffusion cells," *AAPS PharmSciTech*, vol. 15, no. 4, pp. 994–999, 2014, doi: 10.1208/s12249-014-0130-y.

[33] M. Rafiee-Tehrani and A. Mehramizi, "In vitro release studies of piroxicam from oil-in-water creams and hydroalcoholic gel topical formulations," *Drug Dev. Ind. Pharm.*, vol. 26, no. 4, pp. 409–414, 2000, doi: 10.1081/DDC-100101247.

[34] T. Furuishi *et al.*, "Formulation design and evaluation of a transdermal drug delivery system containing a novel eptazocine salt with the Eudragit® E adhesive," *J. Drug Deliv. Sci. Technol.*, vol. 54, no. September, p. 101289, 2019, doi: 10.1016/j.jddst.2019.101289.

[35] I. Jafri, M. H. Shoaib, R. I. Yousuf, and F. R. Ali, "Effect of permeation enhancers on in vitro release and transdermal delivery of lamotrigine from Eudragit®RS100 polymer matrix-type drug in adhesive patches," *Prog. Biomater.*, vol. 8, no. 2, pp. 91–100, 2019, doi: 10.1007/s40204-019-0114-9.

[36] M. Chaturvedi, M. Kumar, K. Pathak, S. Bhatt, and V. Saini, "Surface solid dispersion and solid dispersion of Meloxicam: Comparison and product development," *Adv. Pharm. Bull.*, vol. 7, no. 4, pp. 569–577, 2017, doi: 10.15171/apb.2017.068.

[37] P. Tran, Y. C. Pyo, D. H. Kim, S. E. Lee, J. K. Kim, and J. S. Park, "Overview of the manufacturing methods of solid dispersion technology for improving the solubility of poorly water-soluble drugs and application to

anticancer drugs," *Pharmaceutics*, vol. 11, no. 3, pp. 1–26, 2019, doi: 10.3390/pharmaceutics11030132.

[38] V. Siddharth and G. Sunny, "Formulation and characterization of meloxicam loaded microemulsion for the treatment of rheumatoid arthritis," *World J. Pharm. Res.*, vol. 3, no. 3, pp. 4305–4335, 2014.

[39] V. R. de A. Borges, A. Simon, A. R. C. Sena, L. M. Cabral, and V. P. de Sousa, "Nanoemulsion containing dapsone for topical administration: A study of in vitro release and epidermal permeation," *Int. J. Nanomedicine*, vol. 8, pp. 535–544, 2013, doi: 10.2147/IJN.S39383.

[40] V. A. Borse, A. B. Gangude, and A. B. Deore, "Formulation and evaluation of antibacterial topical gel of doxycycline hyclate, neem oil and tea tree oil," *Indian J. Pharm. Educ. Res.*, vol. 54, no. 1, pp. 206–212, 2020, doi: 10.5530/ijper.54.1.24.

[41] A. Aliyah, W. W. Oktaviana, K. S. Dwipayanti, A. P. Erdiana, R. N. Utami, and A. D. Permana, "Enhanced skin localization of doxycycline using microparticles and hydrogel: Effect of oleic acid as penetration enhancer," *Pharmaciana*, vol. 11, no. 2, p. 239, 2021, doi: 10.12928/pharmaciana.v11i2.21044.

[42] R. K. Chang, A. Raw, R. Lionberger, and L. Yu, "Generic development of topical dermatologic products: Formulation development, process development, and testing of topical dermatologic products," *AAPS J.*, vol. 15, no. 1, pp. 41–52, 2013, doi: 10.1208/s12248-012-9411-0.

[43] N. Mennini, M. Cirri, F. Maestrelli, and P. Mura, "Comparison of liposomal and NLC (nanostructured lipid carrier) formulations for improving the transdermal delivery of oxaprozin: Effect of cyclodextrin complexation," *Int. J. Pharm.*, vol. 515, no. 1–2, pp. 684–691, 2016, doi: 10.1016/j.ijpharm.2016.11.013.

[44] R. Neupane, S. H. S. Boddu, J. Renukuntla, R. J. Babu, and A. K. Tiwari, "Alternatives to biological skin in permeation studies: Current trends and possibilities," *Pharmaceutics*, vol. 12, no. 2, 2020, doi: 10.3390/pharmaceutics12020152.

[45] M. R. Prausnitz and R. Langer, "Transdermal drug delivery," *Nat. Biotechnol.*, vol. 26, no. 11, pp. 1261–1268, 2008, doi: 10.1038/nbt.1504.

[46] P. Mura, M. Bragagni, N. Mennini, M. Cirri, and F. Maestrelli, "Development of liposomal and microemulsion formulations for transdermal delivery of clonazepam: Effect of randomly methylated β-cyclodextrin," *Int. J. Pharm.*, vol. 475, no. 1, pp. 306–314, 2014, doi: 10.1016/j.ijpharm.2014.08.066.

[47] E. Touitou, B. Godin, Y. Karl, S. Bujanover, and Y. Becker, "Oleic acid, a skin penetration enhancer, affects Langerhans cells and corneocytes," *J. Control. Release*, vol. 80, no. 1–3, pp. 1–7, 2002, doi: 10.1016/S0168-3659(02)00004-4.

[48] M. R. Akram, M. Ahmad, A. Abrar, R. M. Sarfraz, and A. Mahmood, "Formulation design and development of matrix diffusion controlled transdermal drug delivery of glimepiride," *Drug Des. Devel. Ther.*, vol. 12, pp. 349–364, 2018, doi: 10.2147/DDDT.S147082.

[49] D. Miron *et al.*, "Influence of penetration enhancers and molecular weight in antifungals permeation through bovine hoof membranes and prediction of efficacy in human nails," *Eur. J. Pharm. Sci.*, vol. 51, no. 1, pp. 20–25, 2014, doi: 10.1016/j.ejps.2013.08.032.

[50] C. Caddeo, O. D. Sales, D. Valenti, A. R. Saurí, A. M. Fadda, and M. Manconi, "Inhibition of skin inflammation in mice by diclofenac in vesicular carriers: Liposomes, ethosomes and PEVs," *Int. J. Pharm.*, vol. 443, no. 1–2, pp. 128–136, 2013, doi: 10.1016/j.ijpharm.2012.12.041.

[51] M. Soniat *et al.*, "Permeation of CO2 and N2 through glassy poly(dimethyl phenylene) oxide under steady- and presteady-state conditions," *J. Polym. Sci.*, vol. 58, no. 9, pp. 1207–1228, 2020, doi: 10.1002/pol.20200053.